Received: 25 June 2024 | Revised: 26 February 2025 | Accepted: 27 February 2025

https://doi.org/10.1016/j.jtha.2025.02.035

ORIGINAL ARTICLE

A glycoprotein VI signaling defect in newly formed platelets generated in stress thrombopoiesis

Stephanie R. Hyslop[1,2] | Jason Corbin[1] | Pradnya Gangatirkar[1] | Marion Lebois[1] | Amanda E. Au[1,2] | Diane Moujalled[1,2] | Irina Pleines[1,2] | Kate D. Sutherland[1,2] | Robert K. Andrews[3] | Elizabeth E. Gardiner[3] | Warren S. Alexander[1,2] | Emma C. Josefsson[1,2,4,5]

[1]The Walter and Eliza Hall Institute of Medical Research, Melbourne, Victoria, Australia

[2]Department of Medical Biology, University of Melbourne, Melbourne, Victoria, Australia

[3]Division of Genome Science and Cancer, John Curtin School of Medical Research, Australian National University, Canberra, Australia

[4]Department of Clinical Chemistry, Region Västra Götaland, Sahlgrenska University Hospital, Gothenburg, Sweden

[5]Department of Laboratory Medicine, Institute of Biomedicine, The University of Gothenburg, Gothenburg, Sweden

Correspondence
Emma C. Josefsson, Department of Clinical Chemistry, Sahlgrenska University Hospital, Bruna stråket 16, 413 45 Gothenburg, Sweden.
Email: emma.josefsson@gu.se

Funding information
National Health and Medical Research Council of Australia Project and Program Grants, Grant/Award Numbers: 1079250 (to E.C.J.) and 1113577 (to W.S.A.); Fellowship, Grant/Award Number: 1058344 (to W.S.A); Investigator, Grant/Award Number: 1173342 (to W.S.A.); Independent Research Institutes Infrastructure Support Scheme Grant, Grant/Award Number: 9000587; and Victorian State Government Operational Infrastructure Support Grant. E.C.J. is the recipient of a fellowship from

Abstract

Background: Newly produced platelets are thought to be more functional than their older counterparts. However, recent work suggests that murine platelets formed following immune-mediated thrombocytopenia possess a transient glycoprotein (GP) VI signaling defect.

Objectives: In this study, we explored whether other models of stress thrombopoiesis would generate platelets that display a functional defect.

Methods: Platelet function was assessed by light transmission aggregometry and/or flow cytometry in genetic and disease models of thrombocytopenia and after chemotherapy-induced thrombocytopenia.

Results: We evaluated platelet function in mice bearing a point mutation in *Bcl-x* and in 2 cancer models, all presenting with thrombocytopenia and a high proportion of reticulated platelets. Flow cytometric analysis of platelet degranulation and integrin activation revealed a significantly diminished response to the GPVI agonist convulxin in all models, but not thrombin. Likewise, platelet aggregation and Syk phosphorylation downstream of GPVI, in response to convulxin, was significantly reduced. Furthermore, a rebound from carboplatin-induced or immune-mediated thrombocytopenia caused a transient GPVI defect. The $Mpl^{-/-}$ model of thrombocytopenia (with a normal proportion of reticulated platelets) was included as a negative control. In response to convulxin, $Mpl^{-/-}$ platelets exhibited normal degranulation and integrin activation.

Conclusion: In this study, we report a functional defect in platelet GPVI signaling present in multiple models of thrombocytopenia that are accompanied by an increased proportion of rapidly generated young platelets. These results indicate that during stress thrombopoiesis, the GPVI receptor becomes entirely functional only after spending some time in circulation.

Manuscript handled by: Ton Lisman

Final decision: Ton Lisman, 27 February 2025

the Lorenzo and Pamela Galli Charitable Trust Australia. S.R.H. is the recipient of an Australian Postgraduate Award from the University of Melbourne.

KEYWORDS
Chemotherapy, immature blood platelets, platelet membrane glycoprotein VI, stress thrombopoiesis, thrombocytopenia

1 | INTRODUCTION

Anucleate platelets are produced from large precursor cells, the megakaryocytes, residing in the bone marrow [1], spleen [2], and lungs [3,4]. The lifespan of platelets in circulation is 5 days in mice and 7 to 10 days in humans. Newly produced platelets are often referred to as reticulated or immature platelets. They are enriched in RNA, often larger is size [5], and are thought to be more reactive than older platelets [6,7]. Clinically, fully automated hematologic analyzers measure the immature (or reticulated) platelet fraction [8], and in research studies, thiazole orange (TO) and Syto 13 are examples of RNA-binding dyes used to label young platelets for flow cytometric analysis [9]. However, in a healthy organism, platelet production is a constant process, and it is a challenge to capture and analyze platelet function in newly formed young platelets, which represent ~10% of a circulating platelet population.

The aging of circulating platelets is an area of research, which has gained much interest in recent years. It is evident that platelets quickly lose function as they age *in vitro*, and hence, platelet storage during blood banking is restricted to 5 to 7 days at room temperature (20-24 °C) in agitated gas permeable bags. *In vivo*, platelet lifespan at steady state is regulated by the intrinsic apoptosis pathway [10,11]. Other mechanisms of platelet clearance include antibody-mediated platelet removal, relevant to immune-mediated thrombocytopenia [12], and platelet desialylation leading to exposure of surface markers that target platelets for clearance from the circulation [13]. In genetically modified mice where platelets are unable to undergo intrinsic apoptosis, due to the absence of death proteins Bak and Bax, platelet half-life and platelet counts are nearly doubled [14]. Hence, these mice provide a model where platelets are aged beyond normal. These mice were found to have reduced hemostatic function, with increased bleeding time and platelets with a lessened ability to release granules [15]. Since the defects could be rescued by synchronizing platelet age, a restriction of platelet lifespan by intrinsic apoptosis is pivotal to maintain a functional hemostatically reactive platelet population [15]. While this finding implies that platelets are removed before they become significantly less reactive, it still does not fully address whether platelet function differs between young and older *in vivo* aged platelets under normal steady state conditions. Results from recent studies, reviewed in [6], demonstrated that physiologic platelet aging is defined by a decline in overall RNA and protein content, concomitant with changes in the transcriptome and proteome. These changes were associated with a reduction in gene ontology terms coupled with platelet functional readouts, including hemostasis, aggregation, and coagulation. A recent study by Veninga et al. [16] examined fractions of large and small platelets separated by centrifugation and identified high glycoprotein (GP) VI protein expression of highly reactive juvenile platelets by flow cytometry, which were mainly found among the large platelet fraction.

Contrary to the view that newly formed platelets are hyperreactive, 2 studies by Gupta et al. [17] and Hardy et al. [18] demonstrated that newly synthesized murine platelets produced after acute, immune-mediated thrombocytopenia exhibited a transient signaling defect in response to the GPVI-specific agonist collagen-related peptide, as well as to collagen and convulxin. Gupta et al. [17] proposed that downregulation of GPVI–immunoreceptor tyrosine–based activation motif signaling in newly formed platelets serves to shield them from activation while traversing the collagen-rich endothelium during their release from megakaryocytes, whereas Hardy et al. [18] speculated that rapid platelet production during acute needs could induce neonatal thrombopoiesis. While research has highlighted the existence of platelet subpopulations based on function, size, and age within patient groups, the common intrinsic changes that occur as platelets age within the circulation are only just being explored. Is there a difference in the function of young platelets produced in steady state conditions versus under stressed conditions with acute needs? In this study, we aimed to explore whether other models of stress thrombopoiesis relevant to human disease or therapy, in addition to immune-induced thrombocytopenia, would generate platelets that display a functional defect.

2 | METHODS

2.1 | Mice

Mpl$^{-/-}$ [19] and *Bcl-x*$^{Plt20/Plt20}$ [11] mice have been previously described. All mice used in this study were bred and housed in conventional clean facilities. All experimental procedures were conducted following Walter and Eliza Hall Institute of Medical Research (WEHI) Animal Ethics Committee approved protocol 2018.012. Mice were euthanized by CO_2 asphyxiation. All mouse strains were maintained on a C57BL/6 background, age and sex matched within experiments. Both male and female mice were used at ages between 7 and 11 weeks. C57BL/6 mice were originally obtained from the Jackson Laboratories and subsequently bred and maintained at WEHI in Melbourne Australia. Notably, *Mpl*$^{-/-}$ mice can be divided into 2 groups displaying low ($136 \pm 19 \times 10^3/\mu L$) or extremely low ($41 \pm 6 \times 10^3/\mu L$) platelet counts [20]. For all experiments using *Mpl*$^{-/-}$ mice, full peripheral blood counts were performed prior to beginning the experiment, and mice displaying extremely low platelet counts were excluded. Mice were rested for 2 weeks prior to blood collection for platelet functional studies.

2.2 | Materials

TO (390062), thrombin (T9326-150UN), PAR4-AP (AYPGKF-NH_2), fibrinogen (F3879), and N-ethylmaleimide were from Sigma-Aldrich. Convulxin (ALX-350-100-C050) was purchased from Enzo Life Sciences and calibration beads 3.5 to 4.0 μm were from Spherotech. Antiplatelet serum (APS) was purchased from Cedarlane. Fluorescently conjugated antibodies included the following: JON/A (integrin αIIbβ3, CD41/CD61 M023-2), GPIX (CD42a, M051-1), GPIbα (CD42b, M040-3), and GPVI (JAQ1, M011-1) from Emfret Analytics; fluorescently conjugated antimouse, αIIb (CD41, MWReg30), anti–P-selectin (CD62P) RB40.34 (561923) from BD Biosciences, and annexin V (A13199) from Life Technologies. Polyclonal rabbit anti–mouse GPVI (intracellular epitope that identifies full-length and remnant cytoplasmic tail domain of GPVI) [21,22], rabbit anti–Syk antibody (2712), and rabbit anti–phospho-Syk antibody (2711) were from Cell Signaling Technology. Direct-blot horseradish peroxidase anti–β-actin was from Sigma-Aldrich, and horseradish peroxidase–conjugated secondary antibodies were from Santa Cruz Biotechnology. Carboplatin was obtained from Pfizer.

2.3 | Murine small cell lung cancer (RP-1) cell line model

A small cell lung cancer cell (SCLC) line was generated from a tumor that formed in the lungs from a mouse on C57BL/6 background, harboring conditional inactivation of retinoblastoma (*Rb)1* and *Trp53* (RP mice) [23] in lung epithelial cells. A lung tumor was minced and cultured in Dulbecco's modified Eagle's medium supplemented with insulin, transferrin, selenium, ethanolamine (1%), epidermal growth factor (200.0 μg/μL), hydrocortisone (0.5 mg/mL), penicillin/streptomycin (1%), and 10% fetal calf serum. Tissue was incubated at 37 °C, 5% CO_2, until cells formed clusters in suspension, at which point they were passaged twice weekly and maintained in the abovementioned medium [24]. For intravenous (i.v.) transplants, single-cell suspensions were prepared, and 5×10^4 cells in 200.0 μL were transplanted into the lateral tail vein per mouse. Mice were sacrificed as a cohort for platelet collection when they reached an ethical end point, when signs of ill health such as weight loss, shivering, hunching, and ruffled fur became apparent.

2.4 | Eμ-*myc* lymphoma mouse model

Primary immature B ($B220^+$, $cKit^-$, IgD^{low}, and IgM^+) Eμ-*myc* lymphoma cells were harvested from lymph nodes and spleen of terminally ill Eμ-*myc* mice on a C57BL/6 background [25]. The harvested cells were then transplanted i.v. via the tail vein into recipient C57BL/6 wild-type mice to generate second-generation Eμ-*myc* lymphoma cells subsequently used in transplant experiments. C57BL/6 mice were injected i.v. with 2×10^4 (5849) or 1 million (5903) second-generation Eμ-*myc* lymphoma cells [26], and mice were euthanized and analyzed at the same time once the first mouse in the experimental cohort reached an ethical end point. Disease severity was measured by peripheral blood counts, spleen, and lymph node (axillary, brachial, inguinal, and mesenteric) weights. Ethical end points included enlarged spleen or lymph nodes detected by palpation, or when signs of ill health such as weight loss, shivering, hunching, and ruffled fur became apparent.

2.5 | Chemotherapy-induced thrombocytopenia

C57BL/6 mice between 8 and 10 weeks of age were injected intraperitoneally (i.p.) with a single dose of carboplatin (100.0 mg/kg) in saline on day 0. Mice were sacrificed in cohorts on day 8, 11, and 16, and blood was collected into microcontainer tubes containing EDTA for peripheral blood counts. Peripheral blood counts were also performed 2 weeks prior to carboplatin treatment. Platelet functional studies and TO staining were performed on day 11 and day 16.

2.6 | Antibody-mediated thrombocytopenia

Acute thrombocytopenia was induced by i.v. injection of 100.0 μL of APS per 20 g body weight (Cedarlane) at a 1:25 predilution. Reticulated platelets were enumerated by TO staining. Platelets were collected at 72 hours (3 days) after APS treatment [15].

2.7 | Flow cytometry analysis of platelet activation

Platelets were isolated from mice as described in Supplementary Methods and resuspended in platelet resuspension buffer to a final concentration of 1×10^8 cells/mL. Platelets where pooled from thrombocytopenic mice to achieve this platelet count. Washed platelets were incubated with convulxin or thrombin or PAR4-AP at several agonist concentrations and antibodies recognizing activated αIIbβ3 (JON/A-PE) and P-selectin fluorescein isothiocyanate in a buffer containing 1mM Ca^{2+} for 20 minutes at room temperature. Samples were diluted in platelet resuspension buffer and analyzed on a FACS Calibur or CytoFLEX with 10 000 events collected in the platelet gate (gating based on forward scatter and side scatter).

2.8 | Measurement of platelet aggregation

Platelets were isolated from mice as described in Supplementary Methods and resuspended in modified Tyrode-HEPES buffer (145.0 mM NaCl, 10.0 mM HEPES, 3.5 mM NaH_2PO_4, 5.0 mM KCl, 2.0 mM $MgCl_2$, 3.0 mg/mL bovine serum albumin, and 10.0 mM glucose, pH 7.4) to a final concentration of 5×10^8 platelets/mL. In a glass aggregometer cuvette, 80.0 μL platelet suspension was added to 160.0 μL modified Tyrode-HEPES buffer supplemented with fibrinogen and 1.0 mM Ca^{2+}. A magnetic stirring bar was placed in the bottom of the cuvette, and

samples were warmed to 37 °C and stirred while light transmission through the platelet suspension was measured in a 4-channel aggregometer (AggRAM; Helena Laboratories); 5.0 μL agonist (thrombin or convulxin) was added to induce aggregation. The percentage aggregation over the course of 8 minutes was recorded. Light transmission through buffer containing platelets and platelet-free buffer was considered 0% and 100%, respectively.

2.9 | TO staining

TO staining was performed on either blood collected from a tail vein bleed or retro-orbital bleed. For tail vein bleeding, 3.0 μL of blood was collected into an EDTA tube containing 14.0 μL resuspension buffer and 3.0 μL Aster-Jandl anticoagulant. TO was prediluted to 1:8570 and αIIb (CD41)-PE to 1:30 in phosphate-buffered saline (PBS); 50.0 μL TO, 10.0 μL αIIb-PE, and 7.0 μL blood was mixed in a FACS tube. For retro-orbital bleeding, heparinized blood was collected in an EDTA tube. TO was prediluted to 1:10 000 and αIIb-PE to 1:30 in PBS; 50.0 μL TO, 10.0 μL αIIb-PE, and 1.0 μL blood was mixed in a FACS tube. All platelet suspensions were incubated at room temperature for 20 minutes in the dark, before 0.4 mL of 1% paraformaldehyde in PBS was slowly added to fix the platelets. Samples were evaluated by flow cytometry (FACScalibur or CytoFLEX), recording 10 000 events in a defined platelet gate. Results were analyzed using FlowJo v10.

2.10 | Statistical analysis

GraphPad PRISM 8.0.2 and 10 was used for statistical analysis. Data are presented as mean ± SEM (unless otherwise stated) for the indicated number of observations. Statistical tests used are indicated in the figure legends. Data distribution normality was assessed in GraphPad PRISM using a Shapiro–Wilk test. For normally distributed data, a 2-tailed Welch *t*-test was used. For nonnormally distributed data, a Mann–Whitney U-test was used to assess statistical significance. A P value of $<.05$ was considered statistically significant.

3 | RESULTS

3.1 | A functional defect in platelets generated after immune-mediated thrombocytopenia

First, we assessed agonist-induced platelet activation by flow cytometry using washed platelets from mice recovering from acute thrombocytopenia induced by antibody-mediated platelet depletion. Wild-type mice were injected i.v. with APS to induce a rapid decrease in circulating platelet counts <10% of steady state. Platelet counts and TO-positive platelets (RNA-containing platelets) were assessed over time before and after platelet depletion, similar to our previous study [15]. In this model, platelet counts remain low (<10% of normal for 24 hours) and then gradually increase. The proportion of young, TO-positive platelets markedly rise (24-hour time point) and then gradually decline to control mice levels (data not shown). We collected platelets on day 3 (72 hours after i.v. injection), when platelet counts had recovered to ∼50% of normal and the %TO-positive platelets were ∼25% (∼8% TO-positive in untreated control mice). Our results agree with those of published work [17,18], showing reduced platelet activation in newly produced murine platelets in response to the GPVI agonist convulxin (Figure 1A, B), but normal to slightly enhanced response to PAR-4 peptide (Figure 1C, D), when assessed by P-selectin exposure and integrin αIIbβ3 (CD41/CD61, GPIIb/IIIa) conformational change (JON/A). We previously characterized platelets at this time point by flow cytometry and found platelets to have slightly increased size and elevated surface receptor levels (including GPVI and PAR-4) [15], in line with published data [17].

3.2 | Mice with genetically modified *Bcl-x* produce platelets with a hemostatic defect

The *Bcl-x*$^{Plt20/Plt20}$ mouse model of thrombocytopenia exhibiting an intrinsic reduction in platelet lifespan due to a mutation in prosurvival Bcl-xL (Plt20) [11]. The mice have a high proportion of young platelets (less than 24 hours old) but normal mean platelet volume (MPV), white blood cell (WBC) count, and red blood cell (RBC) count [11] and provided an excellent tool to evaluate platelet function in newly formed platelets. The prosurvival protein Bcl-x_L is an inhibitor of the intrinsic apoptosis pathway and a major regulator of steady state platelet lifespan [10,11,27]. As expected, *Bcl-x*$^{Plt20/Plt20}$ mice display a platelet count that is 25% of *Bcl-x*$^{+/+}$ control mice (266 ± 6.494 × 10^6 platelets/μL compared with 1097 ± 24.21 × 10^6 platelets/μL) (Figure 2A) and exhibit a significantly increased percentage of TO-positive reticulated platelets (37.660 ± 2.620), compared with *Bcl-x*$^{+/+}$ mice (5.264 ± 0.435) (Figure 2B) [11,20]. After tail tip resection, *Bcl-x*$^{Plt20/Plt20}$ mice exhibited significantly increased time to first stop in bleeding compared with *Bcl-x*$^{+/+}$ littermate controls (306.2 ± 56.96 seconds vs 146.3 ± 33.57 seconds; P = .0267) (Figure 2C). Although not significantly different, there was a trend toward an increased total bleeding time observed in *Bcl-x*$^{Plt20/Plt20}$ mice (333.4 ± 58.93 seconds) compared with that in *Bcl-x*$^{+/+}$ mice (213.8 ± 31.96 seconds) (Supplementary Figure S1). Furthermore, volume of blood loss—derived from measurement of hemoglobin concentration—increased significantly in *Bcl-x*$^{Plt20/Plt20}$ mice (P = .0248) (Figure 2D). As a murine platelet count should generally be <15 × 10^6/μL for a wild-type mouse to exhibit increased or prolonged bleeding [28], we hypothesized that in *Bcl-x*$^{Plt20/Plt20}$, platelets possessed a functional defect, which when combined with moderate thrombocytopenia, contributed to the increased bleeding time.

3.3 | *Bcl-x*$^{Plt20/Plt20}$ platelets are hyporesponsive to GPVI stimulation *in vitro*

Next, we assessed integrin activation and degranulation on washed platelets treated with agonists by flow cytometry. Analysis revealed a

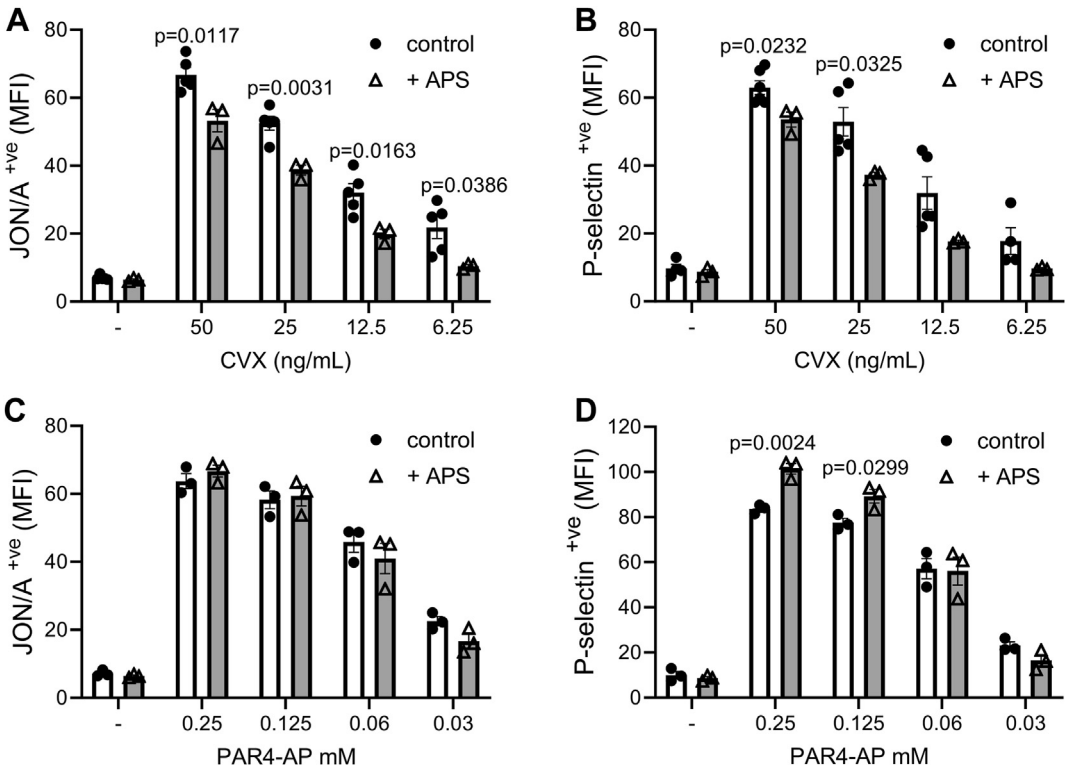

FIGURE 1 Reduced convulxin (CVX)-mediated platelet activation in a rebound from immune thrombocytopenia (A, C) Integrin αIIbβ3 activation (JON/A+) and (B, D) P-selectin exposure following activation with CVX or PAR4-AP on washed platelets from untreated C57BL/6 control mice and 3 days after antiplatelet serum (APS) treatment. Untreated control wild-type mice (n = 3-6) and 3 days after APS treatment (n = 3). Data are expressed as mean fluorescence intensity (MFI). Mean ± SEM. Student's unpaired t-test.

significantly diminished response to the GPVI agonist convulxin in *Bcl-x*$^{Plt20/Plt20}$ platelets (Figure 2E, G), assessed by integrin αIIbβ3 conformational change and surface presentation of P-selectin, while response to PAR-4 stimulation (with thrombin) was only affected at a low dose (0.03 U/mL) (Figure 2F, H). Likewise, platelet light transmission aggregation in response to convulxin stimulation reduced significantly in *Bcl-x*$^{Plt20/Plt20}$ platelets compared with that in *Bcl-x*$^{+/+}$ (Figure 2I, Supplementary Figure S2A), while normal aggregation was observed in response to thrombin stimulation (Figure 2J, Supplementary Figure S2B). These results indicated that the GPVI collagen signaling pathway of platelet activation was affected.

3.4 | *Bcl-x*$^{Plt20/Plt20}$ platelets display defective intracellular GPVI signaling

As GPVI-dependent platelet activation and aggregation was found to be notably affected, we assessed surface expression of GPVI. Analysis by flow cytometry identified no change in the surface expression of GPVI (Figure 2K) or other major surface receptors GPIbα (CD42b), and GPIX (CD42a) in *Bcl-x*$^{Plt20/Plt20}$ platelets (Figure 2L). As GPVI can be metalloproteolyzed, resulting in the release of an ∼55-kDa GPVI fragment and the retention of an intracellular remnant fragment (∼5 kDa) [29], we assessed GPVI expression and cleavage by western blot, using an antibody recognizing an epitope in the mouse GPVI intracellular tail that detects remnant GPVI tail as well as full-length GPVI [21]. As a positive control, washed *Bcl-x*$^{+/+}$ platelets were treated with N-ethylmaleimide, a thiol-modifying reagent that induces GPVI cleavage. Consistent with the flow cytometry results, no change in GPVI expression was seen, and additionally, no cleaved GPVI tail was detected (Figure 2M). Collagen and convulxin activate Src and Syk tyrosine kinases downstream of the GPVI-Fc receptor γ-chain complex, culminating in activation of PLCγ2 [30]. Analysis of downstream GPVI signaling following treatment of washed platelets with increasing concentrations of convulxin revealed a mild defect in Syk phosphorylation following platelet activation with convulxin (Figure 2N, Supplementary Figure S3).

3.5 | Defective GPVI signaling in 2 murine cancer models exhibiting thrombocytopenia

We were interested in exploring whether other models of thrombocytopenia with a high proportion of newly formed immature (TO-positive) platelets would display a similar defect. Two cancer models were selected. In the first, mice develop thrombocytopenia when they display a high burden of liver tumors following i.v. transplantation of RP-1, a SCLC cell line generated from a tumor that formed in the lungs of mice with conditional inactivation of *Rb1* and *Trp53* in lung epithelial cells [23] (Figure 3A). The second model gradually develops

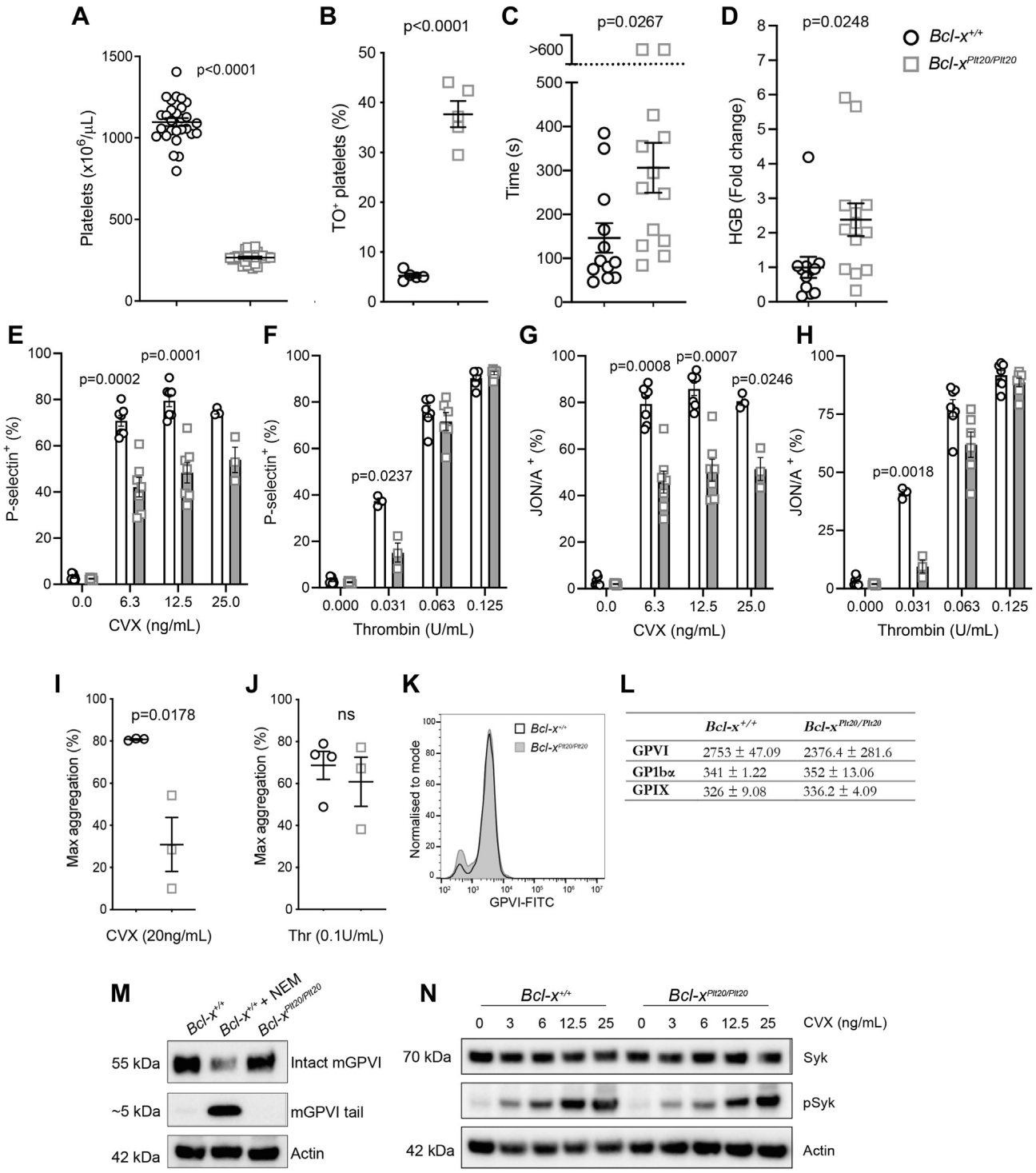

FIGURE 2 Prolonged bleeding time and GPVI signaling defect present in *Bcl-x*$^{Plt20/Plt20}$ mice. (A) Platelet count (n = 25 mice per genotype). (B) Percent thiazole orange–positive platelets (n = 5 mice per genotype) in *Bcl-x*$^{+/+}$ and *Bcl-x*$^{Plt20/Plt20}$ mice. (C) Time to first stop in bleeding (where stop was ≥60 seconds) following 3.0-mm tail tip amputation in *Bcl-x*$^{+/+}$ (n = 12) and *Bcl-x*$^{Plt20/Plt20}$ (n = 13) mice. (D) Hemoglobin content measured from blood collected following 3.0-mm tail tip amputation. Platelet surface P-selectin detected by flow cytometry following activation with convulxin (CVX; E) and thrombin (F). Integrin αIIbβ3 activation (JON/A+) on platelets following activation with CVX (G) and thrombin (H) in *Bcl-x*$^{Plt20/Plt20}$ (n = 3-7) and *Bcl-x*$^{+/+}$ (n = 3-7) mice. Maximum aggregation following activation with 20.0 ng/mL CVX (I) and 0.1 U/mL thrombin (J) in platelets from *Bcl-x*$^{Plt20/Plt20}$and *Bcl-x*$^{+/+}$ mice; each point represents the mean of 3 independent aggregometry runs. (K, L) Surface expression of GPVI, GPIX, and GPIbα on platelets from *Bcl-x*$^{Plt20/Plt20}$ and *Bcl-x*$^{+/+}$ mice by flow cytometry on whole blood. (M) Representative western blot for intact and cleaved GPVI in platelet lysates from *Bcl-x*$^{Plt20/Plt20}$ and *Bcl-x*$^{+/+}$ mice. N-ethylmaleimide (NEM) was used to induce GPVI cleavage in *Bcl-x*$^{+/+}$ platelets. Actin was used as a loading control. (N) Syk and Syk phosphorylation (pSyk) in murine platelets in response to CVX activation shown as representative western blot (n = 3). Actin was used as a loading control. Mean ± SEM. Welch t-test.

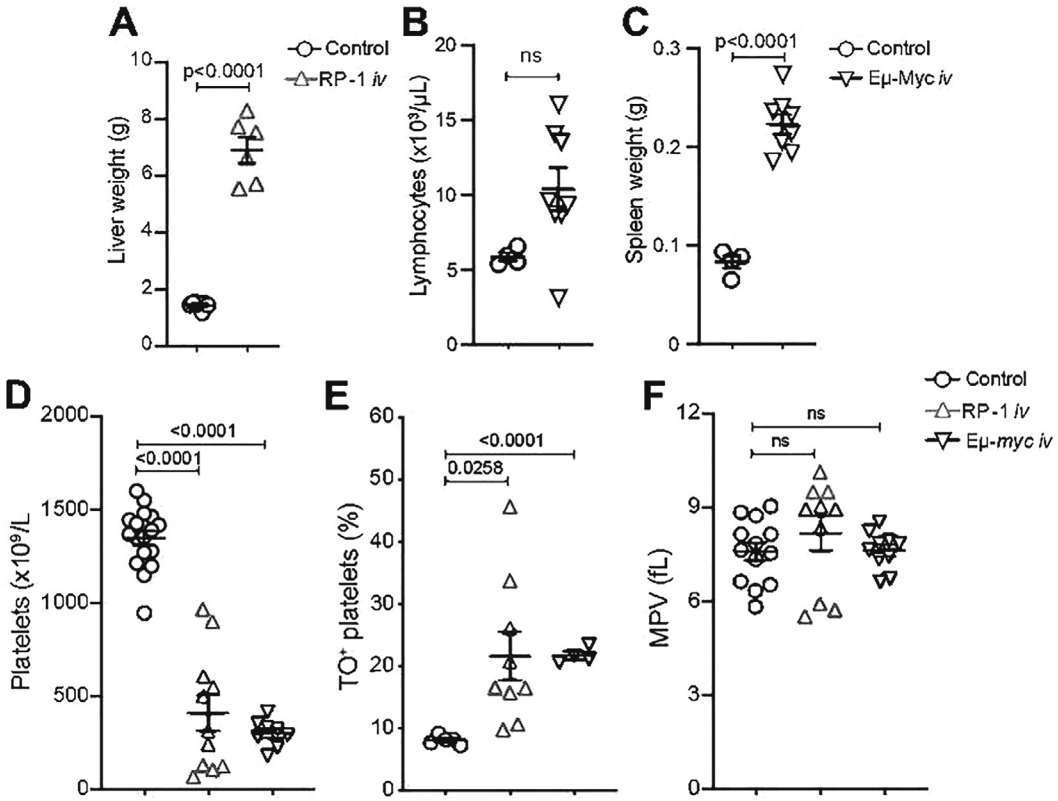

FIGURE 3 Thrombocytopenia associated with increased percentage of reticulated platelets in 2 cancer disease models. (A) Liver weight at 46 days after intravenous (i.v.) injection with RP-1 small cell lung cancer cells (n = 6), compared with nontransplanted C57BL/6 controls (n = 7). (B) Lymphocyte count and (C) spleen weight at 20 days after i.v. injection with Eμ-*myc* lymphoma 5849 cells. (D) Platelet count, (E) percent thiazole orange (TO)–positive platelets, and (F) mean platelet volume (MPV) at 46 days after i.v. injection with RP-1 small cell lung cancer cells (n = 8-11), 20 days after i.v. injection with Eμ-*myc* lymphoma cells (n = 4-10), or in nontransplanted control mice (n = 4-16). Each symbol represents an individual mouse. Mean ± SEM. ns = P >.05. Welch t-test.

thrombocytopenia due to an increased Eμ-*myc* lymphoma burden (assessed by spleen weight and circulating lymphocyte count), following i.v. transplantation of a cell line derived from an Eμ-*myc* transgenic mouse [25] (Figure 3B, C). At the stage of confirmation of significant disease, both models displayed low platelet count (RP-1: 401.4 ± 96.39 × 10^6 platelets/μL; Eμ-*myc*: 292.5 ± 26.23 × 10^6 platelets/μL) (Figure 3D) and a high percentage of reticulated platelets (RP-1: 21.54 ± 3.906, Eμ-*myc*: 21.55 ± 0.6252) (Figure 3E). Platelet size, assessed by MPV, was not significantly different from control platelets in either model (Figure 3F).

Assessing the response of platelets from the RP-1 transplantable model of SCLC, to convulxin or thrombin stimulation, revealed the same phenotype as the *Bcl-x*$^{Plt20/Plt20}$ mice with a platelet defect observed in response to convulxin but not thrombin, for activation assessed by flow cytometry (P-selectin exposure and integrin conformational change) and platelet aggregation (Figure 4A–F, Supplementary Figure S4A, B). Additionally, surface GPVI and GPIbα expression—assessed by flow cytometry—was normal (Figure 4G, H). As with the *Bcl-x*$^{Plt20/Plt20}$ platelets, no GPVI cleavage was detectable by western blot (Figure 4I), and Syk phosphorylation following convulxin treatment was reduced compared with that in nontransplanted control mice (Figure 4J, Supplementary Figure S5).

Platelets from mice transplanted with the Eμ-*myc* cell line also displayed a diminished response to convulxin when assessing activation by flow cytometry and aggregation (Figure 5A, C, E, Supplementary Figure S6A); however, in contrast to the previous models, we also observed a slight reduction in the response to thrombin (Figure 5B, D, F, Supplementary Figure S6B). Additionally, reduced expression of GPVI was detected by flow cytometry and western blot, although no GPVI cleaved fragment was detected (Figure 5G–I, Supplementary Figure S7), in agreement with a study reporting reduced GPVI surface levels on platelets from patients with lymphoproliferative diseases [31]. Other platelet surface receptors (GPIbα, GPIX, and αIIb/CD41) were unaffected (Figure 5H, Supplementary Figure S7). As with the previous 2 models, Syk phosphorylation reduced in response to convulxin stimulation in platelets from mice transplanted with the Eu-*myc* cell line, compared with that in nontransplanted controls (Figure 5J, Supplementary Figure S8). Together, this indicated a 2-fold GPVI defect in the lymphoma model, with both reduced GPVI surface expression and dysfunctional intracellular signaling contributing to the observed phenotype.

In all 3 models, the bone marrow megakaryocyte numbers were abnormal. However, while *Bcl-x*$^{Plt20/Plt20}$ [11,20,27] and RP-1 tumor–bearing mice displayed significantly elevated megakaryocyte

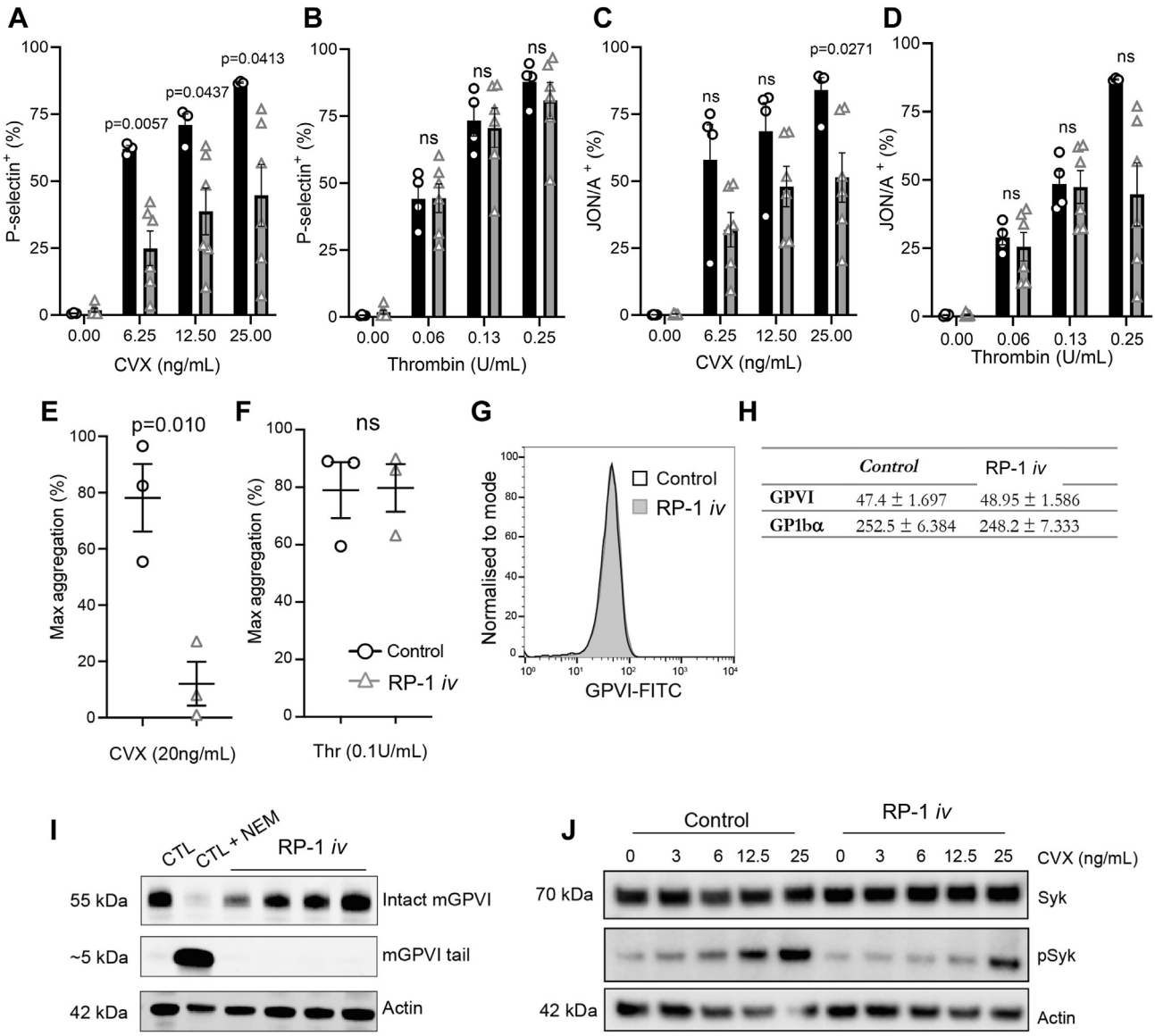

FIGURE 4 Reduced convulxin (CVX)-mediated platelet activation and aggregation in platelets from mice bearing RP-1 small cell lung cancer (SCLC) tumors. Platelet surface P-selectin detected by flow cytometry following activation with convulxin (CVX, A) and thrombin (B). Integrin αIIbβ3 activation (JON/A+) on platelets following activation with CVX (C) and thrombin (D) in control (nontransplanted) (n = 4) and RP-1 tumor–bearing (n = 6) mice. Maximum aggregation following activation with 20.0 ng/mL CVX (E) and 0.1 U/mL thrombin (F) in platelets from control (nontransplanted) and RP-1 tumor–bearing mice; each point represents the mean of 3 independent aggregometry runs. (G,H) Surface expression of GPVI and GPIbα on platelets from RP-1 SCLC tumor–bearing mice compared with control mice by flow cytometry on whole blood. (I) Representative western blot for intact and cleaved GPVI in platelet lysates from RP-1 tumor–bearing mice and nontransplanted control mice. N-ethylmaleimide (NEM) was used to induce GPVI cleavage in control (CTL) platelets. Actin was used as a loading control. (J) Syk and Syk phosphorylation (pSyk) in platelets in response to CVX activation shown as representative western blot (n = 3). Actin was used as a loading control. ns = P >.05; Mean ± SEM. Welch t-test.

numbers, indicating enhanced platelet production in response to accelerated platelet clearance (Supplementary Figure S9), mice transplanted with the Eμ-*myc* lymphoma cell line had reduced megakaryocyte numbers likely due to bone marrow lymphocyte overproliferation and subsequent overcrowding leading to abnormal platelet production (Supplementary Figure S9). Despite the different mechanisms of thrombocytopenia in these models, a similar functional defect in platelet GPVI signaling was observed.

3.6 | The GPVI defect is due to an increased percentage of immature platelets

We wanted to evaluate whether the findings resulted from an enhanced proportion of newly produced platelets rather than from being produced in the setting of thrombocytopenia. To explore this, we used the well-characterized $Mpl^{-/-}$ model of severe thrombocytopenia [19]. These mice lack the thrombopoietin (TPO) receptor

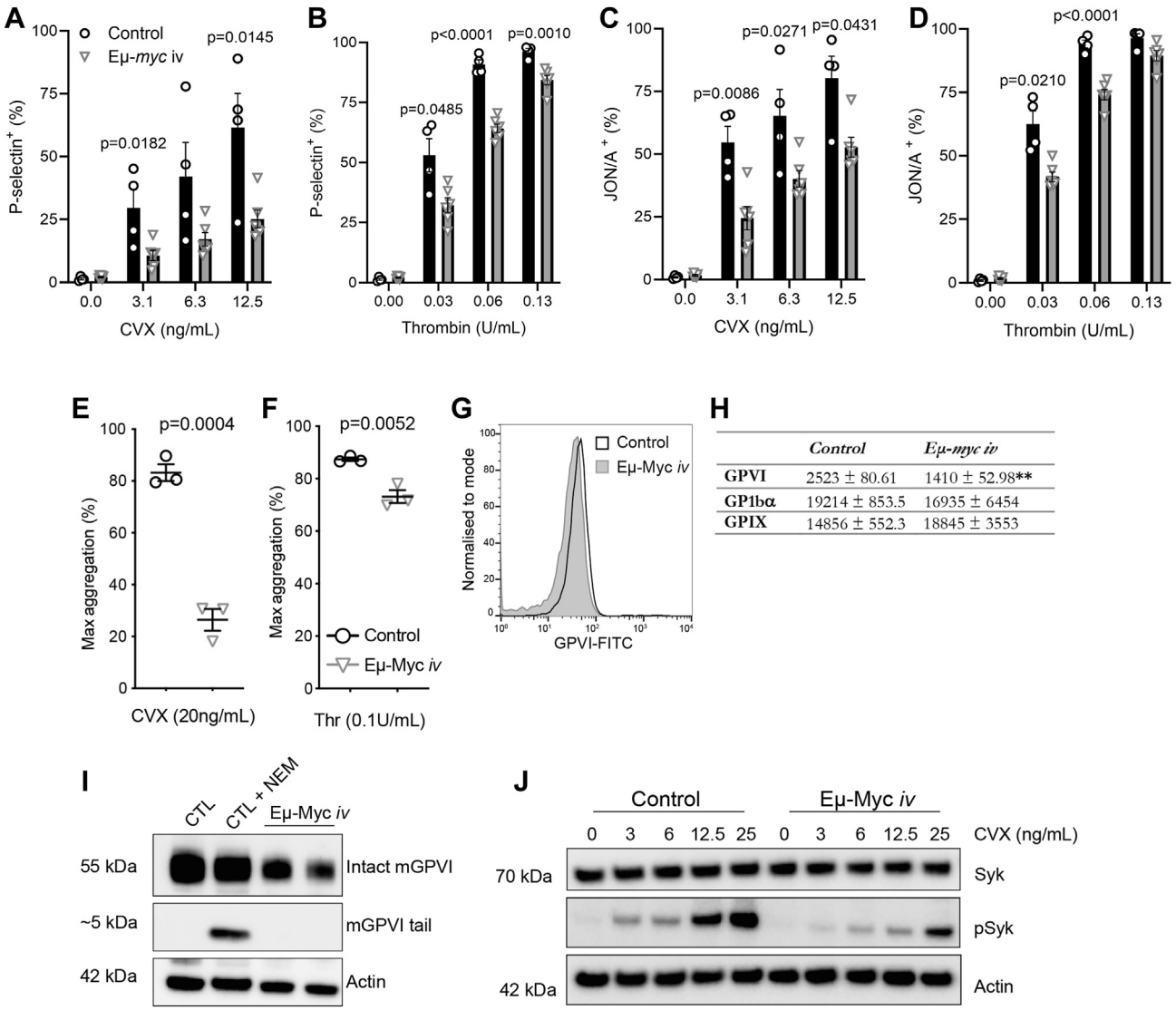

FIGURE 5 Reduced activation and aggregation of platelets derived from lymphomic Eμ-*myc* mice. Platelet P-selectin detected by flow cytometry following activation with convulxin (CVX; A) and thrombin (B). Integrin $\alpha_{IIb}\beta_3$ activation (JON/A+) on platelets following activation with CVX (C) and thrombin (D) in control (nontransplanted; $n = 4$) and Eμ-*myc* 5849 tumor–bearing ($n = 6$) mice. Maximum platelet aggregation following activation with 20.0 ng/mL CVX (E) and 0.1 U/mL thrombin (F) of platelets from control and Eμ-*myc* tumor–bearing mice; each point represents the mean of 3 independent aggregometry runs. (G,H) Surface expression of GPVI, GPIX, and GPIbα on platelets from Eμ-*myc* 5849 tumor–bearing mice compared with control mice by flow cytometry on whole blood. (I) Western blot for intact and cleaved GPVI in platelet lysates from Eμ-*myc* tumor–bearing and nontransplanted mice. N-ethylmaleimide (NEM) was used to induce GPVI cleavage in control (CTL) platelets. (J) Syk and Syk phosphorylation (pSyk) in platelets in response to CVX activation shown as representative western blot ($n = 2$). Actin was used as a loading control. Mean ± SEM. Welch *t*-test.

c-Mpl, resulting in reduced platelet production with low numbers of megakaryocytes and progenitor cells and a platelet count approximately 10% of $Mpl^{+/+}$ control mice (Figure 6A). Unlike $Bcl\text{-}x^{Plt20/Plt20}$ mice, $Mpl^{-/-}$ mice maintain an unaltered percentage of reticulated platelets (Figure 6B), with slightly increased MPV (Figure 6C). Assessing platelet activation in response to convulxin and thrombin by flow cytometry revealed no activation change in response to convulxin stimulation compared with that in wild-type controls (Figure 6D, F). Interestingly, however, as with the platelets in the Eμ-*myc* lymphoma model, there was a reduced activation response to thrombin-mediated PAR stimulation (Figure 6E, G). As a similar GPVI signaling defect was observed in 4 models of thrombocytopenia with increased immature platelet proportions ($Bcl\text{-}x^{Plt20/Plt20}$, 2 cancer models and immune-mediated thrombocytopenia), it seemed likely that this defect was present only in models that generate increased proportions of immature platelets.

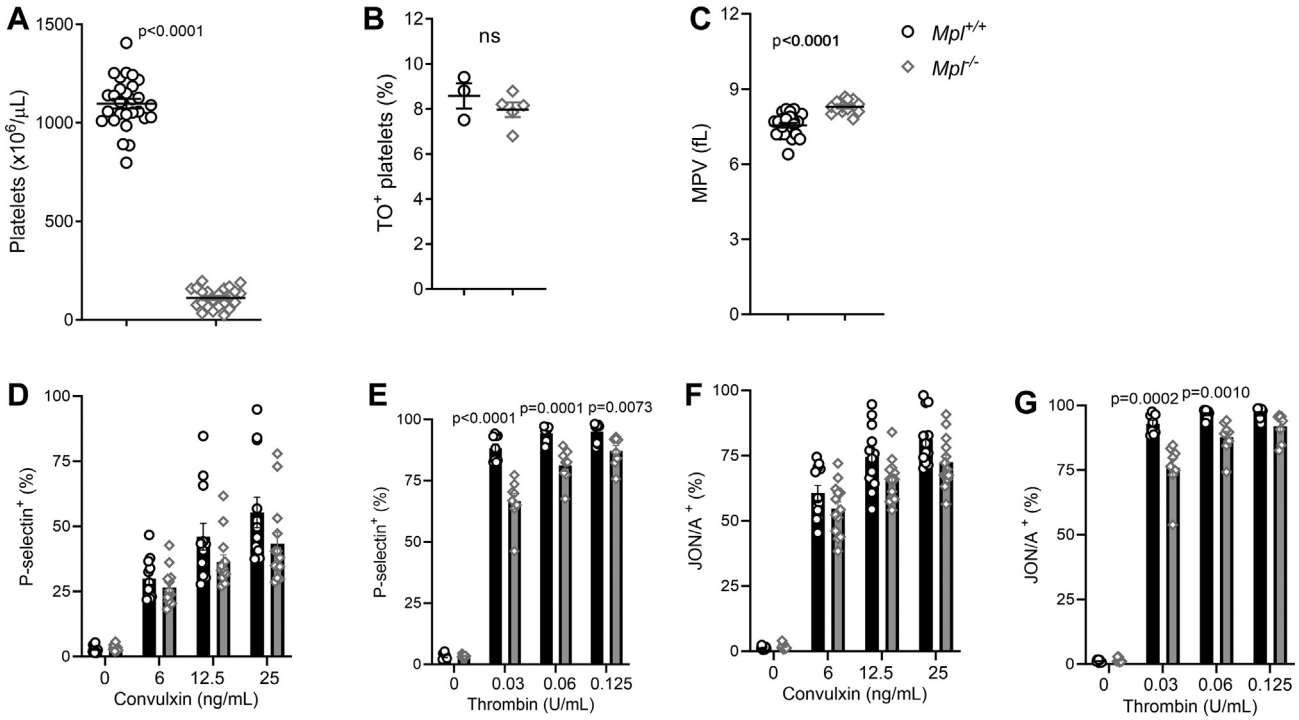

FIGURE 6 Normal response to convulxin (CVX)-mediated activation in platelets from $Mpl^{-/-}$ mice. (A) Platelet count (n = 28 mice per genotype), (B) percent thiazole orange (TO)–positive platelets (n = 3-5), and (C) MPV of platelets (n = 28 mice per genotype) from $Mpl^{+/+}$ and $Mpl^{-/-}$ mice. Each symbol represents an individual mouse. Platelet P-selectin detected by flow cytometry following activation with CVX (D) and thrombin (E). Integrin $\alpha_{IIb}\beta_3$ activation (JON/A+) on platelets following activation with CVX (F) and thrombin (G) in $Mpl^{+/+}$ (n = 9) and $Mpl^{-/-}$ (n = 8) mice. Mean ± SEM. Welch t-test. ns = P >.05.

3.7 | Platelet activation defect is present following chemotherapy-induced thrombocytopenia

Chemotherapy-induced thrombocytopenia (CIT) is a serious complication for cancer patients [32], and loss or reduction of GPVI signaling could further contribute to the increased bleeding events observed in patients with CIT. Carboplatin is among the chemotherapy agents known to cause CIT [33] by killing both megakaryocytes and their progenitors [34]. We examined whether the GPVI signaling defect would be present in newly produced platelets following carboplatin-induced thrombocytopenia. C57Bl/6 mice were administered (100.0 mg/kg) carboplatin i.p., and platelet count was measured on days 8, 11, and 16 (Figure 7A, B). By days 8 to 11 following carboplatin treatment, the platelet count dropped significantly (157 ± 145 × 10^6 platelets/μL on day 8 and 131± 102 × 10^6 platelets/μL on day 11 compared with untreated control, 1367 ± 78 × 10^6 platelets/μL; P < .0001) (Figure 7A, B), and the percentage of TO-positive platelets notably increased (45.5% ± 3.6% TO+ on day 11; P < .0001) (Figure 7C) compared with that in untreated controls (10.1% ± 1.7%). On day 11 these mice also displayed a significantly increased MPV and reduced WBC and RBC counts (Figure 7D–F). By day 16, the platelet count had markedly risen compared with that on day 11 but was still significantly lower than that in untreated control mice (741 ± 206 × 10^6 platelets/μL; P = .0005) (Figure 7A, B). The percentage of TO-positive platelets was also elevated, but not to the same extent as the day 11 time point (22.6% ± 10.6% TO+ day 16; P = .0190) (Figure 7C). MPV, WBC, and RBC levels had all returned to normal by this time point (Figure 7D–F). Flow cytometry analysis revealed a significantly diminished response to both convulxin and thrombin in platelets collected at day 11 time point compared with that in untreated controls; however, the response in platelets collected on day 16 had returned to normal (Figure 7G–J). Together, these results indicated that GPVI signaling–induced platelet activation was transiently compromised in newly formed platelets after carboplatin-induced thrombocytopenia in mice. Furthermore, thrombin-induced platelet activation was also affected.

3.8 | Procoagulant platelet activity in *Bcl-x*$^{Plt20/Plt20}$ platelets

Finally, we assessed whether there were functional consequences of these defective immature platelets, beyond the reduced response to GPVI stimulation. For this, we assessed whether this defect impacted the formation of procoagulant platelets in *Bcl-x*$^{Plt20/Plt20}$ mice. Procoagulant platelets expose phosphatidylserine (PS) on their surface and provide a surface for assembly of coagulation complexes, leading to efficient generation of thrombin and fibrin formation [35]. Defective procoagulant platelet activity is associated with clinical bleeding disorders such as Scott syndrome, in which surface exposure of PS is compromised [36]. Consequently, thrombin generation is impaired,

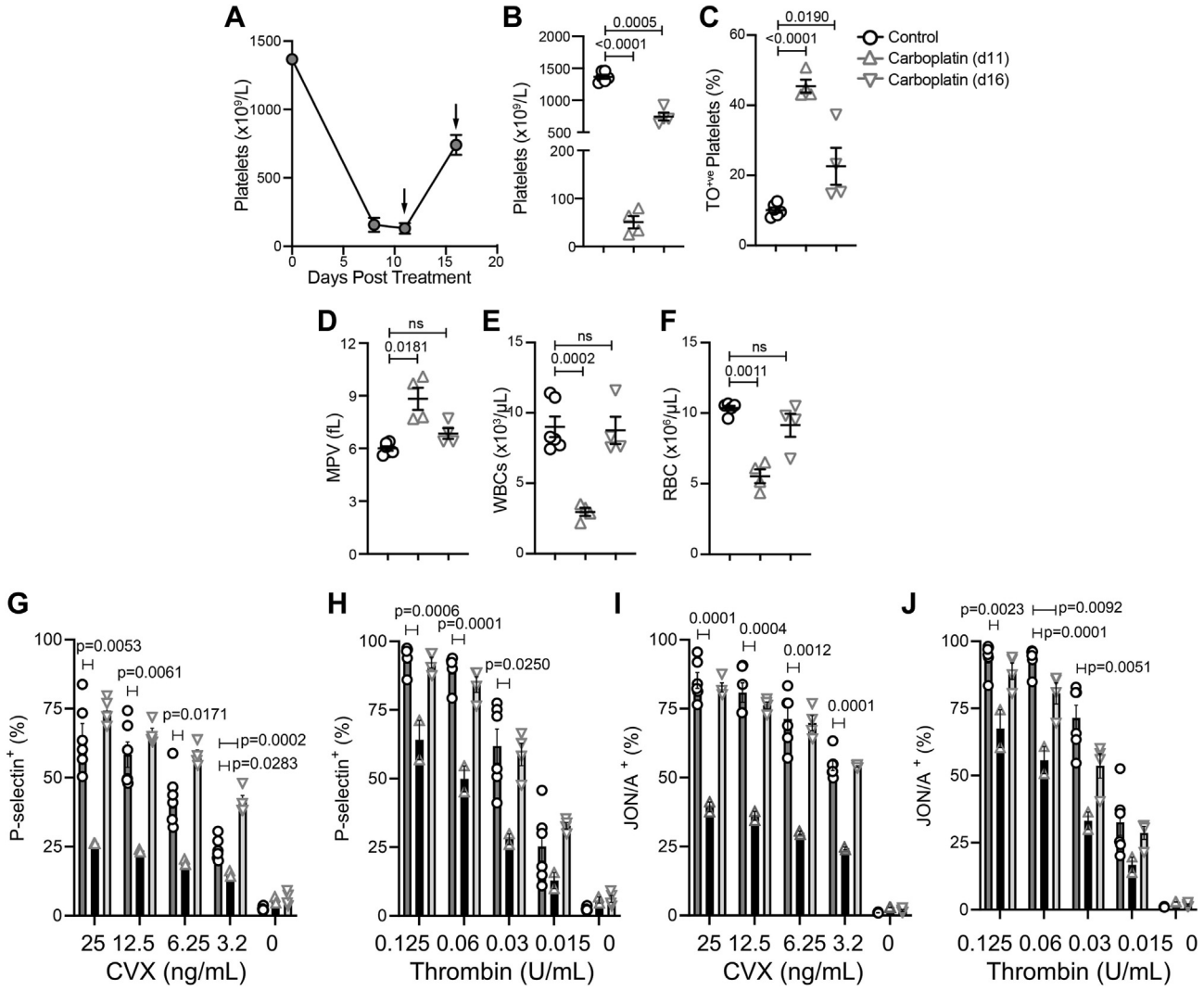

FIGURE 7 Platelet activation defect following carboplatin-induced thrombocytopenia. (A) Platelet count over time following carboplatin 100.0 mg/kg intraperitoneal (i.p.) treatment on day 0; $n = 6$ mice, before treatment; $n = 8$ mice, day 8; $n = 7$ mice, day 11; and $n = 8$ mice, day 16 after carboplatin treatment. Arrows indicate time points at which platelets were collected for further analysis. (B) Platelet count, (C) percent thiazole orange (TO)-positive platelets, (D) mean platelet volume (MPV), (E) white blood cell (WBC) count, and (F) red blood cell (RBC) count at days 11 and 16 after carboplatin treatment ($n = 4$) and in nontreated control mice ($n = 8$). Platelet surface P-selectin detected by flow cytometry following activation with convulxin (CVX; G) and thrombin (H). Integrin αIIbβ3 activation (JON/A+) on platelets following activation with CVX (I) and thrombin (J) at days 11 and 16 after carboplatin treatment (d11, $n = 2$, pooled from 4 mice; d16, $n = 4$) and in nontreated control mice ($n = 6$). *P* values are calculated as relative to control, mean ± SEM. Welch *t*-test.

and patients display hemostatic abnormalities [35]. As GPVI response to collagen promotes the formation of procoagulant platelets and thrombin generation [37], we investigated whether procoagulant activity was impaired in platelets from *Bcl-x*$^{Plt20/Plt20}$ mice. Following dual activation with convulxin and thrombin of washed platelets from *Bcl-x*$^{+/+}$ and *Bcl-x*$^{Plt20/Plt20}$ mice, we observed no difference in the level of PS exposure on the platelet surface (assessed by annexin-V and P-selectin double-positive platelets) (Supplementary Figure S10), indicating that the procoagulant activity of platelets was not affected in these mice. P-selectin was included in the antibody mix to ensure that we were measuring highly activated procoagulant platelets, and not those undergoing apoptosis [27] in accordance with a recent communication from the International Society on Thrombosis and Haemostasis SSC on platelet physiology and vascular biology [38]. Taken together, the data reported in this study define a functional GPVI signaling defect present in newly formed platelets, in conditions of stress thrombopoiesis, which affects bleeding time in the setting of moderate thrombocytopenia but not procoagulant activity when assessed *in vitro*.

4 | DISCUSSION

Consistent with studies by Gupta et al. [17] and Hardy et al. [18], we provide evidence that newly formed young platelets released after antibody-mediated thrombocytopenia in mice display a GPVI defect

resulting in impaired convulxin-dependent activation. Importantly, we identified a similar mechanism with a selective GPVI–immunoreceptor tyrosine–based activation motif signaling defect downstream of GPVI in 3 mouse models of thrombocytopenia (*Bcl-x*$^{Plt20/Plt20}$, RP-1 SCLC, and Eμ-*myc* lymphoma) with a large proportion of young platelets (21%-38% TO positive). Convulxin-dependent GPVI activation led to reduced platelet aggregation, degranulation, and integrin conformational change, as well as reduced phosphorylation of Syk (in a setting of normal Syk levels). Since platelet GPVI surface expression was normal in the *Bcl-x*$^{Plt20/Plt20}$, and SCLC models, this indicated a signaling defect downstream of GPVI. In line with data from patients with lymphoproliferative diseases [31], platelet surface GPVI reduced slightly in the murine lymphoma model, which could have further contributed to a lessened convulxin response in that model.

We included the *Mpl*$^{-/-}$ model of severe thrombocytopenia with a normal pool of TO-positive platelets to investigate whether the mechanism applied to all thrombocytopenias, independent of them harboring an increased proportion of reticulated platelets. Our results demonstrated that convulxin-induced platelet degranulation and integrin conformational change were normal in *Mpl*$^{-/-}$ platelets. This result implicates a selective GPVI defect in newly produced platelets, detected only in thrombocytopenias associated with an increased proportion of reticulated platelets.

As the transplantable model of SCLC used in this study is characterized by numerous large tumors in the liver, it is likely that the observed thrombocytopenia develops because of liver dysfunction. The liver produces TPO and clears aged platelets, making it a major regulator of the number of platelets in circulation. In chronic liver disease, TPO synthesis is reduced and platelet destruction in the spleen is increased, resulting in thrombocytopenia in many patients [39,40]. Importantly, although thrombocytopenia is common in patients with liver disease, it is rarely severe; however, platelet function is often affected [41]. It is possible that a platelet functional defect like that identified in the SCLC model in this study could be present in patients with liver disease or hepatocellular carcinoma. Interestingly, collagen-induced platelet aggregation is reduced in patients with cirrhosis [42,43].

We further investigated platelet function in the rebound phase from carboplatin-induced thrombocytopenia, a condition relevant to patients with cancer receiving platinum chemotherapy. Carboplatin targets progenitor cells and megakaryocytes, leading to thrombocytopenia after a few days of treatment followed by rebound thrombocytosis. We found a transient defect in convulxin-induced platelet activation on day 11 (when the reticulated platelets were 45.5%), that normalized on day 16. Schoenwaelder et al. [44] previously demonstrated that Bcl-xL-inhibitory BH3 mimetics, developed for cancer therapy, can prompt a transient thrombocytopathy that weakens the hemostatic function of platelets. Mechanistically, Bcl-xL-inhibition induces rapid thrombocytopenia due to platelet apoptosis, followed by rebound thrombocytosis. Interestingly, marked defects in collagen-related peptide–induced platelet P-selectin expression and integrin activation were observed 2 hours after administration of the Bcl-2 family inhibitor ABT-263, despite only subtle changes in GPVI levels, in keeping with our results generated in the CIT model. Furthermore, the results from the study by Schoenwaelder et al. [44] agree with the outcomes from the *Bcl-x*$^{Plt20/Plt20}$ model, where the mechanism of thrombocytopenia is similar, although has reached a steady state.

Mechanistically, it is tempting to speculate that a transient GPVI defect in newly produced platelets would protect them from activation when being released from megakaryocytes and in close contact with subendothelial collagen [17], followed by a rapid maturation process of the platelet surface receptor in circulation. It is currently unclear whether this mechanism only applies to conditions of rapid platelet generation in acute needs or whether this applies to all newly produced platelets but with differences in kinetics. In a healthy individual, the newly produced reticulated platelet population is ~10%, and it is technically challenging to assess platelet function in this rather small population and with the potentially added interference with RNA dyes. Progress with new labeling techniques [9,45,46],and specific markers of young platelets [16,47] is being made, and future studies should be able to assess platelet function in diluted whole blood collected from patients during the recovery phase from immune-mediated thrombocytopenia and CIT, clinical conditions with a large proportion of rapidly produced reticulated platelets. A recent study by Veninga et al. [16] identified, among the large platelets, a highly reactive juvenile platelet subpopulation with high GPVI expression, which could also be found in patients with immune-mediated thrombocytopenia. In future studies it would be interesting to further dissect changes to the GPVI receptor and downstream signaling pathways on a molecular level that might exist in a newly produced platelets, compared with receptors on a circulating aged population. Provenzale et al. [48] recently revealed a resetting of the protein phosphorylation profile in platelets exposed to endothelium that may contribute to platelet inhibition. It is tempting to speculate that a similar type of mechanism would transiently keep GPVI in an immature hyporeactive version during rapid platelet production, before conversion to a fully functional receptor.

There are limitations when performing platelet function testing in the setting of thrombocytopenia, affecting results obtained from both light transmission aggregometry and flow cytometry [49,50]. In this study, in order to avoid this issue, we adjusted the washed platelet counts to be the same in the groups compared for the agonist-induced platelet activation experiments by flow cytometry and aggregometry (ie, washed platelets were pooled from several mice in the setting of thrombocytopenia when needed).

In summary, we confirmed that newly formed young murine platelets display a transient defect resulting in impaired convulxin-dependent activation. Importantly, this mechanism was not present in all thrombocytopenias, but only identified in thrombocytopenias accompanied with a significantly increased proportion of newly synthesized platelets including CIT and immune-induced thrombocytopenia, 2 thrombocytopenic cancer models, and the *Bcl-x*$^{Plt20/Plt20}$ model with enhanced platelet turnover due to platelet apoptosis. Future studies will evaluate whether the same platelet signaling defect can be observed in platelets from patients experiencing a rebound from a thrombocytopenic episode. Our findings could

potentially be of importance for managing diseases or drug treatments that include a rebound from thrombocytopenia.

ACKNOWLEDGMENTS

We thank Prof Benjamin Kile for providing *Bcl-x*$^{Plt20/Plt20}$ mice and Keti Stoev, Nicole Lynch, Stephanie Bound, Jasmine McManus, and Janelle Lochland at WEHI for outstanding technical assistance.

AUTHOR CONTRIBUTIONS

S.R.H. designed and performed research, analyzed data, prepared figures, and wrote the paper. E.C.J. conceived, designed, and supervised research and wrote the paper. J.C., P.G., M.L., A.E.A., D.M., and I.P. conducted experiments and analyzed data. K.D.S., W.S.A., R.K.A., and E.E.G. contributed to intellectual discussions of the data and provided reagents. All authors reviewed the paper.

DECLARATION OF COMPETING INTERESTS

There are no competing interests to disclose.

ORCID

Emma C. Josefsson https://orcid.org/0000-0001-6478-5204

REFERENCES

[1] Asquith NL, Carminita E, Camacho V, Rodriguez-Romera A, Stegner D, Freire D, Becker IC, Machlus KR, Khan AO, Italiano JE. The bone marrow is the primary site of thrombopoiesis. *Blood*. 2024;143:272–8.

[2] Valet C, Magnen M, Qiu L, Cleary SJ, Wang KM, Ranucci S, Grockowiak E, Boudra R, Conrad C, Seo Y, Calabrese DR, Greenland JR, Leavitt AD, Passegué E, Méndez-Ferrer S, Swirski FK, Looney MR. Sepsis promotes splenic production of a protective platelet pool with high CD40 ligand expression. *J Clin Invest*. 2022;132:e153920. https://doi.org/10.1172/JCI153920

[3] Lefrançais E, Ortiz-Muñoz G, Caudrillier A, Mallavia B, Liu F, Sayah DM, Thornton EE, Headley MB, David T, Coughlin SR, Krummel MF, Leavitt AD, Passegué E, Looney MR. The lung is a site of platelet biogenesis and a reservoir for haematopoietic progenitors. *Nature*. 2017;544:105–9.

[4] Davenport P, Liu ZJ, Sola-Visner M. Fetal vs adult megakaryopoiesis. *Blood*. 2022;139:3233–44.

[5] Dowling MR, Josefsson EC, Henley KJ, Hodgkin PD, Kile BT. Platelet senescence is regulated by an internal timer, not damage inflicted by hits. *Blood*. 2010;116:1776–8.

[6] Allan HE, Vadgama A, Armstrong PC, Warner TD. Platelet ageing: a review. *Thromb Res*. 2023;231:214–22.

[7] Armstrong PC, Hoefer T, Knowles RB, Tucker AT, Hayman MA, Ferreira PM, Chan MV, Warner TD. Newly formed reticulated platelets undermine pharmacokinetically short-lived antiplatelet therapies. *Arterioscler Thromb Vasc Biol*. 2017;37:949–56.

[8] Buttarello M, Mezzapelle G, Freguglia F, Plebani M. Reticulated platelets and immature platelet fraction: clinical applications and method limitations. *Int J Lab Hematol*. 2020;42:363–70.

[9] Hille L, Cederqvist M, Hromek J, Stratz C, Trenk D, Nührenberg TG. Evaluation of an alternative staining method using SYTO 13 to determine reticulated platelets. *Thromb Haemost*. 2019;119:779–85.

[10] Josefsson EC. Platelet intrinsic apoptosis. *Thromb Res*. 2023;231:206–13.

[11] Mason KD, Carpinelli MR, Fletcher JI, Collinge JE, Hilton AA, Ellis S, Kelly PN, Ekert PG, Metcalf D, Roberts AW, Huang DCS, Kile BT. Programmed anuclear cell death delimits platelet life span. *Cell*. 2007;128:1173–86.

[12] González-López TJ, Provan D, Bárez A, Bernardo-Gutiérrez A, Bernat S, Martínez-Carballeira D, Jarque-Ramos I, Soto I, Jiménez-Bárcenas R, Fernández-Fuertes F. Primary and secondary immune thrombocytopenia (ITP): time for a rethink. *Blood Rev*. 2023;61:101112.

[13] Falet H, Rivadeneyra L, Hoffmeister KM. Clinical impact of glycans in platelet and megakaryocyte biology. *Blood*. 2022;139:3255–63.

[14] Josefsson EC, James C, Henley KJ, Debrincat MA, Rogers KL, Dowling MR, White MJ, Kruse EA, Lane RM, Ellis S, Nurden P, Mason KD, O'Reilly LA, Roberts AW, Metcalf D, Huang DCS, Kile BT. Megakaryocytes possess a functional intrinsic apoptosis pathway that must be restrained to survive and produce platelets. *J Exper Med*. 2011;208:2017–31.

[15] Pleines I, Lebois M, Gangatirkar P, Au AE, Lane RM, Henley KJ, Kauppi M, Corbin J, Cannon P, Bernardini J, Alwis I, Jarman KE, Ellis S, Metcalf D, Jackson SP, Schoenwaelder SM, Kile BT, Josefsson EC. Intrinsic apoptosis circumvents the functional decline of circulating platelets but does not cause the storage lesion. *Blood*. 2018;132:197–209.

[16] Veninga A, Handtke S, Aurich K, Tullemans BME, Brouns SLN, Schwarz SL, Heubel-Moenen FCJI, Greinacher A, Heemskerk JWM, van der Meijden PEJ, Thiele T. GPVI expression is linked to platelet size, age, and reactivity. *Blood Adv*. 2022;6:4162–73.

[17] Gupta S, Cherpokova D, Spindler M, Morowski M, Bender M, Nieswandt B. GPVI signaling is compromised in newly formed platelets after acute thrombocytopenia in mice. *Blood*. 2018;131:1106–10.

[18] Hardy AT, Palma-Barqueros V, Watson SK, Malcor JD, Eble JA, Gardiner EE, Blanco JE, Guijarro-Campillo R, Delgado JL, Lozano ML, Teruel-Montoya R, Vicente V, Watson SP, Rivera J, Ferrer-Marín F. Significant hypo-responsiveness to GPVI and CLEC-2 agonists in pre-term and full-term neonatal platelets and following immune thrombocytopenia. *Thromb Haemost*. 2018;118:1009–20.

[19] Alexander WS, Roberts AW, Nicola NA, Li R, Metcalf D. Deficiencies in progenitor cells of multiple hematopoietic lineages and defective megakaryocytopoiesis in mice lacking the thrombopoietic receptor c-Mpl. *Blood*. 1996;87:2162–70.

[20] Lebois M, Dowling MR, Gangatirkar P, Hodgkin PD, Kile BT, Alexander WS, Josefsson EC. Regulation of platelet lifespan in the presence and absence of thrombopoietin signaling. *J Thromb Haemost*. 2016;14:1882–7.

[21] Bishton MJ, Gardiner EE, Harrison SJ, Prince HM, Johnstone RW. Histone deacetylase inhibitors reduce glycoprotein VI expression and platelet responses to collagen related peptide. *Thromb Res*. 2013;131:514–20.

[22] Gardiner EE, Karunakaran D, Shen Y, Arthur JF, Andrews RK, Berndt MC. Controlled shedding of platelet glycoprotein (GP)VI and GPIb-IX-V by ADAM family metalloproteinases. *J Thromb Haemost*. 2007;5:1530–7.

[23] Sutherland KD, Proost N, Brouns I, Adriaensen D, Song JY, Berns A. Cell of origin of small cell lung cancer: inactivation of Trp53 and Rb1 in distinct cell types of adult mouse lung. *Cancer Cell*. 2011;19:754–64.

[24] Best SA, Hess JB, Souza-Fonseca-Guimaraes F, Cursons J, Kersbergen A, Dong X, Rautela J, Hyslop SR, Ritchie ME, Davis MJ, Leong TL, Irving L, Steinfort D, Huntington ND, Sutherland KD. Harnessing natural killer immunity in metastatic SCLC. *J Thorac Oncol*. 2020;15:1507–21.

[25] Adams JM, Harris AW, Pinkert CA, Corcoran LM, Alexander WS, Cory S, Palmiter RD, Brinster RL. The c-myc oncogene driven by immunoglobulin enhancers induces lymphoid malignancy in transgenic mice. *Nature*. 1985;318:533–8.

[26] Au AE, Corbin J, Lebois M, Gangatirkar P, Yassinson F, Hyslop SR, Cannon P, Mason KD, Li-Wai-Suen CSN, Garnham AL, Moujalled D, Cimmino L, Alexander WS, Josefsson EC. Proinflammatory microenvironment promotes lymphoma progression in mice with high megakaryocyte and TPO levels. *Blood Adv*. 2023;7:1560–71.
[27] Zhang H, Nimmer PM, Tahir SK, Chen J, Fryer RM, Hahn KR, Iciek LA, Morgan SJ, Nasarre MC, Nelson R, Preusser LC, Reinhart GA, Smith ML, Rosenberg SH, Elmore SW, Tse C. Bcl-2 family proteins are essential for platelet survival. *Cell Death Differ*. 2007;14:943–51.
[28] Morowski M, Vögtle T, Kraft P, Kleinschnitz C, Stoll G, Nieswandt B. Only severe thrombocytopenia results in bleeding and defective thrombus formation in mice. *Blood*. 2013;121:4938–47.
[29] Gardiner EE, Andrews RK. Platelet receptor expression and shedding: glycoprotein Ib-IX-V and glycoprotein VI. *Transfus Med Rev*. 2014;28:56–60.
[30] Nieswandt B, Watson SP. Platelet-collagen interaction: is GPVI the central receptor? *Blood*. 2003;102:449–61.
[31] Qiao J, Schoenwaelder SM, Mason KD, Tran H, Davis AK, Kaplan ZS, Jackson SP, Kile BT, Andrews RK, Roberts AW, Gardiner EE. Low adhesion receptor levels on circulating platelets in patients with lymphoproliferative diseases before receiving Navitoclax (ABT-263). *Blood*. 2013;121:1479–81.
[32] Weycker D, Hatfield M, Grossman A, Hanau A, Lonshteyn A, Sharma A, Chandler D. Risk and consequences of chemotherapy-induced thrombocytopenia in US clinical practice. *BMC Cancer*. 2019;19:151.
[33] Kuter DJ. Managing thrombocytopenia associated with cancer chemotherapy. *Oncology (Williston Park)*. 2015;29:282–94.
[34] Zeuner A, Signore M, Martinetti D, Bartucci M, Peschle C, De Maria R. Chemotherapy-induced thrombocytopenia derives from the selective death of megakaryocyte progenitors and can be rescued by stem cell factor. *Cancer Res*. 2007;67:4767–73.
[35] Battinelli EM. Procoagulant platelets: not just full of hot air. *Circulation*. 2015;132:1374–6.
[36] van Geffen JP, Swieringa F, Heemskerk JW. Platelets and coagulation in thrombus formation: aberrations in the Scott syndrome. *Thromb Res*. 2016;141(Suppl 2):S12–6.
[37] Lecut C, Feijge MA, Cosemans JM, Jandrot-Perrus M, Heemskerk JW. Fibrillar type I collagens enhance platelet-dependent thrombin generation via glycoprotein VI with direct support of alpha2beta1 but not alphaIIbbeta3 integrin. *Thromb Haemost*. 2005;94:107–14.
[38] Josefsson EC, Ramström S, Thaler J, Lordkipanidzé M, COAGAPO study group. Consensus report on markers to distinguish procoagulant platelets from apoptotic platelets: communication from the Scientific and Standardization Committee of the ISTH. *J Thromb Haemost*. 2023;21:2291–9.
[39] Barsam SJ, Psaila B, Forestier M, Page LK, Sloane PA, Geyer JT, Villarica GO, Ruisi MM, Gernsheimer TB, Beer JH, Bussel JB. Platelet production and platelet destruction: assessing mechanisms of treatment effect in immune thrombocytopenia. *Blood*. 2011;117:5723–32.
[40] Peck-Radosavljevic M. Thrombocytopenia in liver disease. *Can J Gastroenterol*. 2000;14(Suppl D):60d–6d.
[41] Lisman T, Luyendyk JP. Platelets as modulators of liver diseases. *Semin Thromb Hemost*. 2018;44:114–25.
[42] Vinholt PJ, Hvas AM, Nielsen C, Söderström AC, Sprogøe U, Fialla AD, Nybo M. Reduced platelet activation and platelet aggregation in patients with alcoholic liver cirrhosis. *Platelets*. 2018;29:520–7.
[43] Lecchi A, Tosetti G, Ghali C, La Marca S, Clerici M, Padovan L, Femia EA, Primignani M, La Mura V, Lampertico P, Peyvandi F, Tripodi A. Comprehensive investigation of platelet function in patients with cirrhosis. *Thromb Res*. 2024;237:64–70.
[44] Schoenwaelder SM, Jarman KE, Gardiner EE, Hua M, Qiao J, White MJ, Josefsson EC, Alwis I, Ono A, Willcox A, Andrews RK, Mason KD, Salem HH, Huang DCS, Kile BT, Roberts AW, Jackson SP. Bcl-xL-inhibitory BH3 mimetics can induce a transient thrombocytopathy that undermines the hemostatic function of platelets. *Blood*. 2011;118:1663–74.
[45] Armstrong PC, Allan HE, Kirkby NS, Gutmann C, Joshi A, Crescente M, Mitchell JA, Mayr M, Warner TD. Temporal in vivo platelet labeling in mice reveals age-dependent receptor expression and conservation of specific mRNAs. *Blood Adv*. 2022;6:6028–38.
[46] Josefsson EC, White MJ, Dowling MR, Kile BT. Platelet life span and apoptosis. *Methods Mol Biol*. 2012;788:59–71.
[47] Angénieux C, Dupuis A, Gachet C, de la Salle H, Maître B. Cell surface expression of HLA I molecules as a marker of young platelets. *J Thromb Haemost*. 2019;17:1511–21.
[48] Provenzale I, Solari FA, Schönichen C, Brouns SLN, Fernández DI, Kuijpers MJE, van der Meijden PEJ, Gibbins JM, Sickmann A, Jones C, Heemskerk JWM. Endothelium-mediated regulation of platelet activation: Involvement of multiple protein kinases. *FASEB J*. 2024;38:e23468.
[49] Boknäs N, Macwan AS, Södergren AL, Ramström S. Platelet function testing at low platelet counts: When can you trust your analysis? *Res Pract Thromb Haemost*. 2019;3:285–90.
[50] Jourdi G, Ramström S, Sharma R, Bakchoul T, Lordkipanidzé M. FC-PFT in TP study group. Consensus report on flow cytometry for platelet function testing in thrombocytopenic patients: communication from the SSC of the ISTH. *J Thromb Haemost*. 2023;21:2941–52.

SUPPLEMENTARY MATERIAL

The online version contains supplementary material available at https://doi.org/10.1016/j.jtha.2025.02.035